ROBotic Open-architecture Technology for
Cognition, Understanding and Behavior

Project No. 004370

RobotCub
Development of a Cognitive Humanoid Cub

Instrument:	Integrated Project
Thematic Priority:	IST - Cognitive Systems

5.2 Implementation of visual recognition and imitation of goal-directed reaching motion.

Due date: **01/09/2005 (+45 days)**
Submission Date: **04/10/2005**

Start date of project: **01/09/2004**

Duration: **60 months**

Organisation name of lead contractor for this deliverable: **EPFL**

Responsible Person: **Prof. A. Billard**

Revision: **1.0**

Project co-funded by the European Commission within the Sixth Framework Programme (2002-2006)		
Dissemination Level		
PU	Public	**PU**
PP	Restricted to other programme participants (including the Commission Service)	
RE	Restricted to a group specified by the consortium (including the Commission Service)	
CO	Confidential, only for members of the consortium (including the Commission Service)	

Contents

1 Introduction

This deliverable reports on work conducted at EPFL, UH and IST, as part of WP5 - Task 2 *Early Imitation Behavior*. Throughout this WP, we take a developmental and biological stance to imitation. Here, we report on efforts aiming at defining the necessary skills for performing simple visuo-motor imitation of goal-directed reaching motions, such as those displayed by a typicaly developping child of about 18 months, see Deliverable D2.1. At this age, the child is still clumsy in her grasping skills, but already very precise in her reaching motions. Imitation is inherent to the child's development and, at 18 months, the child is capable of immediate and robust imitation of goal-directed motion [1, 2].
In this report, we present results on implementing basic skills for imitation in a humanoid robot. UH investigates the role that turn-taking, approach-avoidance and other social skills play in setting up the interaction dynamics necessary to imitation. EPFL develops biologically plausible controllers for supporting visuo-motor reaching at the same level of dexterity as observed in human reaching motion and extends this to simple visuo-motor imitation of goal-directed motion. IST investigates how this visuo-motor mapping may be acquired during development and how it can then be extended to support an understanding of the self-generated motion and their effect on the world. This mechanisms can then further drive imitation of simple sequences of reaching and grasping actions.

2 EPFL Contribution to task 5.2: A Model of Reaching Movements

In this report, we present a model of reaching movements, which produces smooth trajectories and can adapt online to external perturbations, such as sudden displacements of the target. This model is then used in an imitation framework, allowing a robot to reach to the object to which a human demonstrator is reaching.

2.1 Introduction

The control of human reaching movements seems to rely on several distinct yet redundant representations of the motion [7] [6], see also deliverable (D 5.1). Moreover, it has been argued that the dynamical systems theory is an attractive framework for explaining and accounting for the variability and the robustness observed in human reaching motions [10] [15].
The model described below combines those two elements (redundant representation and dynamical systems) in order to achieve a higher robustness and adaptability.

2.2 The VITE model

The VITE model for reaching movements was originally developed by Bullock and Grossberg [3]. This model describes the muscle control, and beside it being consistent with neurobiological data, several general characteristics of human reaching movements such as the asymmetric bell-shaped velocity profile, the speed-accuracy tradeoff law can be derived from it.

In a slightly modified version, the VITE model can be expressed by the following equation:

$$\ddot{\mathbf{r}} = \alpha(-\dot{\mathbf{r}} + \beta(\mathbf{r_T} - \mathbf{r})) \tag{1}$$

where $\mathbf{r}$ is the present position vector, $\mathbf{r_T}$ is the target position vector and α, β are scalars between 0 and 1. It can be easily verified that this dynamical system creates a stable attractor at the target location, and that the present position will reach the target with a straight line and a roughly bell-shaped velocity profile and stay there.

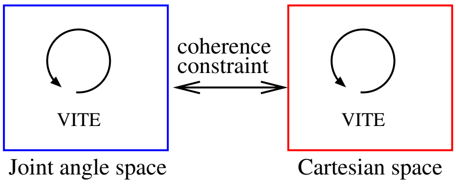

Figure 1: A schematic representation of the model.

2.3 A multimodal control model

The model of reaching motions can be schematically represented as in figure 1. It is composed of two parallel VITE controllers, one active in the 3D hand location space (or cartesian space) and one active in the joint angle space (or arm configuration space). Of course, those two controllers cannot be completely independent one from another because a particular arm configuration corresponds to a particular hand location. Hence, coherence constraints between the two controllers are necessary.
Let $\theta_{\mathbf{t}} \in \Re^{\mathbf{n}}$ and $\mathbf{x}_{\mathbf{t}} \in \Re^{\mathbf{m}}$ denote respectiveley the arm configuration and the hand location at time t, where n is the number of degrees-of-freedom (dof) and m the dimension of the external space (3 in general). Then the coherence constraints are enforced in the following way: If the system is in position $(\theta_{\mathbf{t}}, \mathbf{x}_{\mathbf{t}})$ at time t, the two VITE controllers will bring it to the desired position $(\theta^{\mathbf{d}}_{\mathbf{t+1}}, \mathbf{x}^{\mathbf{d}}_{\mathbf{t+1}})$ at time $t+1$. This desired arm configuration being in general incompatible with the desired hand location, the system is brought to position $(\theta_{\mathbf{t+1}}, \mathbf{x}_{\mathbf{t+1}})$ which is closest to the desired position, while remaining compatible. This can be expressed by a constrained optimization problem and solved using the classical Lagrange multipliers technique:

$$\underset{\theta,\mathbf{x}}{\mathrm{Min}} \quad \frac{1}{2}\big((\theta-\theta^{\mathbf{d}})^{\mathbf{T}}\mathbf{W}^{\theta}(\theta-\theta^{\mathbf{d}}) + (\mathbf{x}-\mathbf{x}^{\mathbf{d}})^{\mathbf{T}}\mathbf{W}^{\mathbf{x}}(\mathbf{x}-\mathbf{x}^{\mathbf{d}})\big) \quad \mathrm{u.c.} \quad \mathbf{x} = \mathbf{K}(\theta), \tag{2}$$

where the time index $t+1$ has been dropped. In this formula K is the kinematic function and the diagonal matrices $W^{\theta} \in \Re^{n\times n}$ and $W^{x} \in \Re^{m\times m}$ control the influence of each of the controllers.
The solution of this constraint optimization problem is given by:

$$\theta_{\mathbf{t+1}} = \theta_{\mathbf{t}} + (\mathbf{W}^{\theta} + \mathbf{J}^{\mathbf{T}}\mathbf{W}^{\mathbf{x}}\mathbf{J})^{-\mathbf{1}}\big(\mathbf{J}^{\mathbf{T}}\mathbf{W}^{\mathbf{x}}(\mathbf{x}^{\mathbf{d}}_{\mathbf{t+1}} - \mathbf{x}_{\mathbf{t}}) + \mathbf{W}^{\theta}(\theta^{\mathbf{d}}_{\mathbf{t+1}} - \theta_{\mathbf{t}})\big), \tag{3}$$

where $J \in \Re^{n\times m}$ is the Jacobian of the kinematic function K. By modifying the two parameters W^{θ} and W^{x}, one can vary the control strategy from a pure cartesian control ($W^{\theta} = 0$) to a pure joint angle control ($W^{x} = 0$).

2.3.1 Variations on the model

In order to increase the smoothness of the trajectories and avoid that the system bumps into its joint boundaries, a couple of variations of the model were studied. The first variation was obtained by introducing a **rest position** in the workspace center towards which the system would be attracted. This can be expressed by adding a term to the cost function to minimize:

$$\underset{\theta,\mathbf{x}}{\mathrm{Min}} \quad \frac{1}{2}\big((\theta-\theta^{\mathbf{d}})^{\mathbf{T}}\mathbf{W}^{\theta}(\theta-\theta^{\mathbf{d}}) + (\mathbf{x}-\mathbf{x}^{\mathbf{d}})^{\mathbf{T}}\mathbf{W}^{\mathbf{x}}(\mathbf{x}-\mathbf{x}^{\mathbf{d}}) + (\theta-\theta^{\mathbf{r}})^{\mathbf{T}}\mathbf{W}^{\mathbf{r}}(\theta-\theta^{\mathbf{r}})\big) \quad \mathrm{u.c.} \quad \mathbf{x} = \mathbf{K}(\theta), \tag{4}$$

where $W^{r}(\theta)$ is proportional to the squared distance to the target, so that the rest term reduces to zero when the system reaches its target.

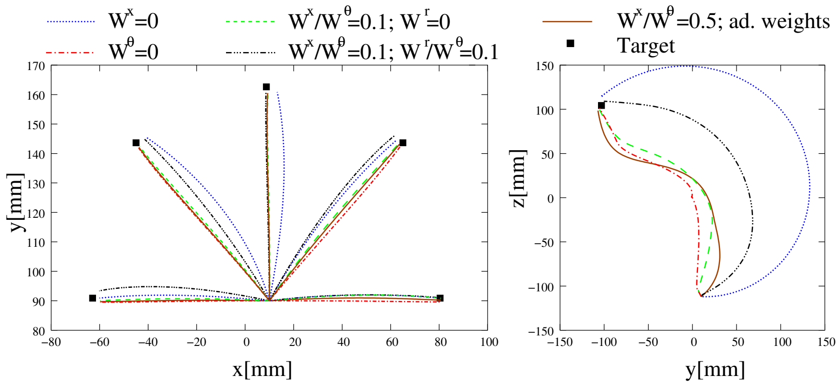

Figure 2: Left: the trajectories in a horizontal plane for movements in the center of the workspace. Right: trajectories for a movement nearby workspace boundaries. The various trajectories correspond to various versions of the controller. For the adaptive weight version (ad. weight) the weight quotient is the valid for the center of the workspace only

The second variation is motivated by the observation that the working space is convex when expressed in joint angle coordinates but not when expressed in cartesian coordinates. This means that, unlike a purely cartesian control, a purely angular control will never bump into the workspace boundaries and will always be smooth. The idea of the second variation is therefore to gradually move to a joint angle control when approaching the workspace boundaries in order to keep the trajectory smooth, thus having **adaptive weights**. This can be achieved by making the weights dependent on the arm configuration as follows:

$$\frac{w_t^x}{w_t^\theta} = \frac{1}{2}A\Big(-\cos\big(2\pi \cdot \frac{(\theta_t - \theta_{min})}{\theta_{max} - \theta_{min}}\big) + 1\Big), \tag{5}$$

where w_t^x and w_t^θ correspond respectively to a cartesian and angular weight at a given time t, θ_{min} and θ_{max} are the corresponding joint angle boundaries, θ_t is the corresponding angular position at time t and A is a constant setting the maximum value for w^x/w^θ. By applying this formula, the control is purely angular ($w^x = 0$) when the system is on the joint boundary.

2.4 Results

Several versions of the controller were tested on simulations. The purely angular version (dotted), the purely cartesian version (dashed-dotted), the multimodal version (dashed), the multimodal version with rest position (dashed-ellipsis), and the multimodal version where weights adapt to angular position (solid). Two kinds of motions were tested, movements that lie in the center of the workspace (Figure 2 left) and movement nearby the workspace boundaries (reaching behind the robot's neck, Figure 2 right). The joint angle position, velocity and acceleration of the trajectories depicted on Figure 2 right are shown on Figure 3. One can see that, as expected, the purely cartesian controller has a very jerky velocity and acceleration, while the purely angular controller is very smooth.
In order to evaluate the various trajectories, the integral of the squared jerk (i.e. derivative of the acceleration) of the hand trajectory was taken. This cost functional, which was suggested as being optimized by human reaching motions [9], provides a good measure of the smoothness of the trajectory, and also penalizes long trajectories. Figure 4 shows the results. One can see that the best controller is the one with adaptive weights (solid diamonds) and approximately equal base weights. Indeed, by looking at Figures 2 and 3 one can see that this controller provides smooth trajectories (solid) and relatively short

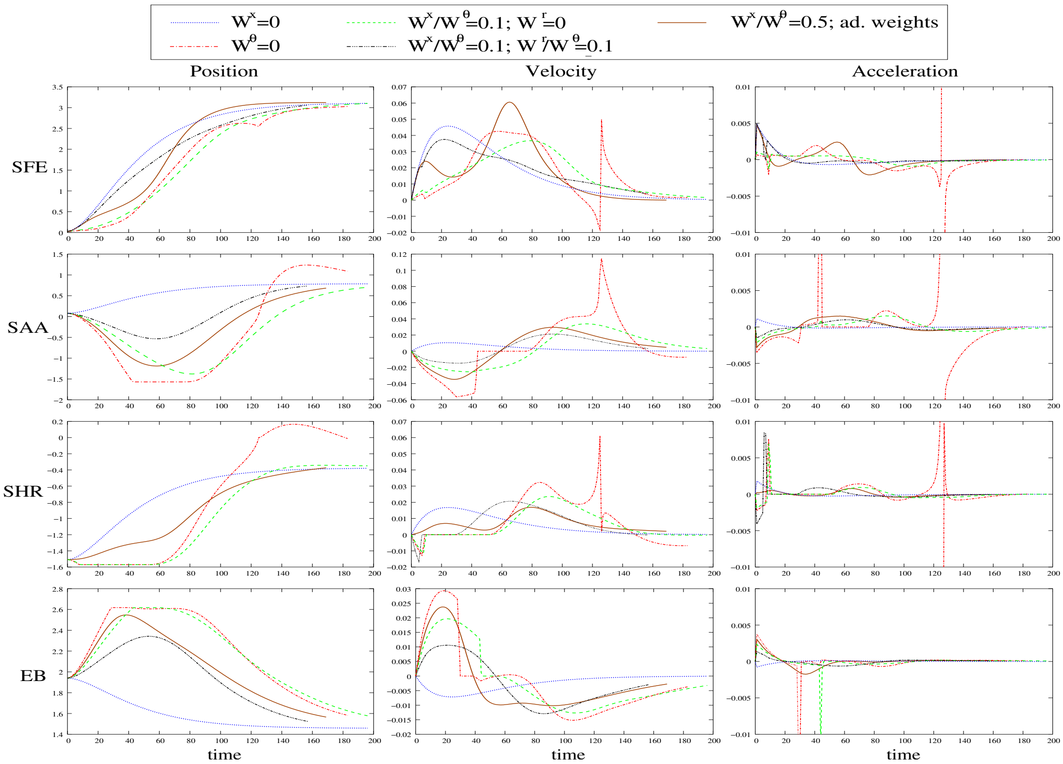

Figure 3: Angle position, velocity and acceleration for the movement depicted in Figure 2 right for various versions of the controller. The blue line corresponds to a purely angular controller, the red one to a purely cartesian controller (traditional pseudo-inverse algorithm), the green line to a mixed controller, the black line to a mixed controller with rest position, and the brown line to a mixed controller with adaptive weights. The four rows (SFE, SAA, SHR and EB) correspond to the four dofs of the robotic arm.

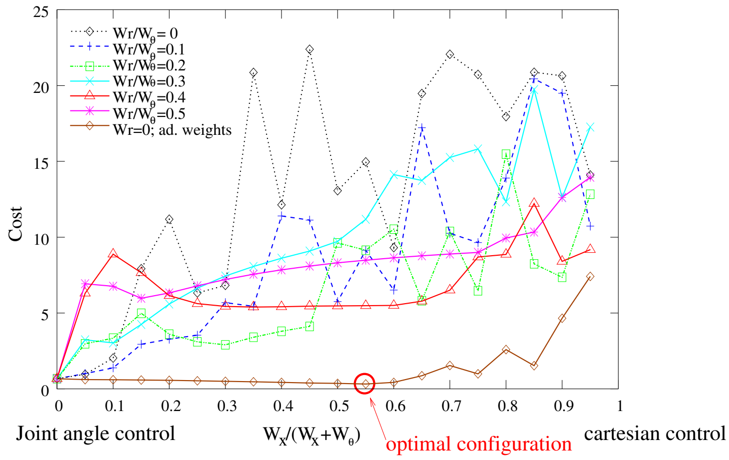

Figure 4: The value of the integral of the squared jerk for the movement of Figure 2 right for various parameters. The abscissa represents the cartesian controller's influence. The different lines correspond to different influences of the rest position.

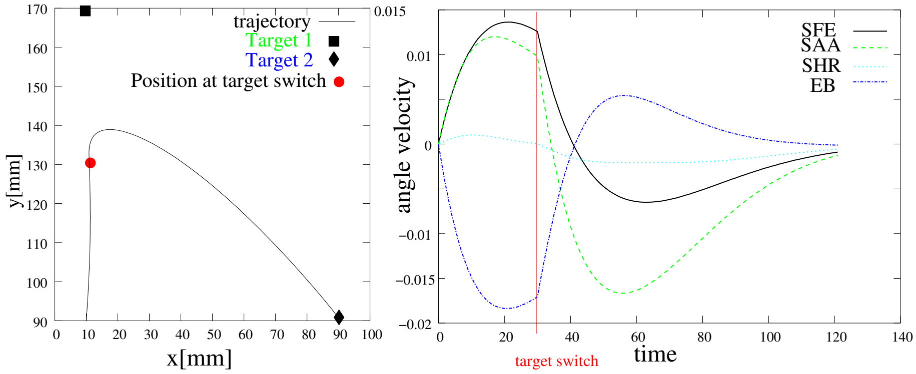

Figure 5: Left: the hand path by a switch of target during reaching remains smooth. Right: the corresponding joint angle velocities are continuous.

hand paths. This is due to the fact that this controller behaves like the purely joint angle controller nearby workspace boundaries (thus having its smoothness) and like the purely cartesian controller in the center of the workspace (thus producing short hand paths).

Because the VITE model is a dynamical system with an attractor point at the target location, it is very robust to external perturbations. And because it is a linear second-order system, the speed is guaranteed to be continuous by a sudden change of target location. This fact is illustrated in figure 5, when one can see the trajectory of the arm reaching for a given location, and a sudden switch of the target. The arm smoothely adapts its trajectory to reach the new target.

2.5 Implementation

The model is implemented on the Hoap2 humanoid robot of Fujitsu operated by RealTime Linux. This robot has a four dof arm, but this is not a limitation of our model, which can be adapted to any kind of arm. A stereovision system continuously tracks the position of the target. This position is then used by

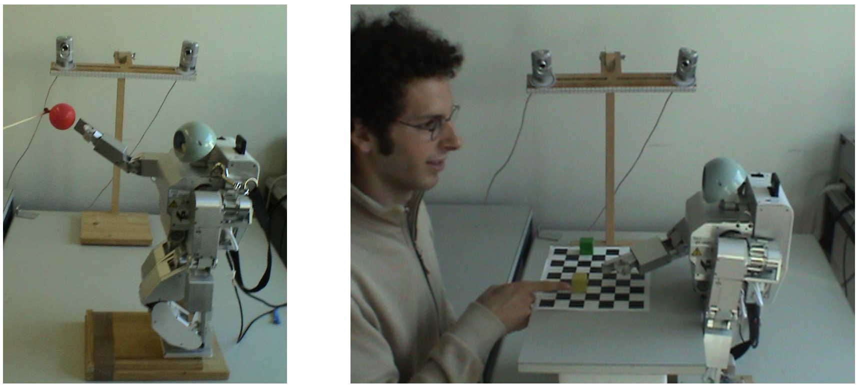

Figure 6: Left: The experimental reaching setup. A stereovision system tracks the target and the robot reaches for it. Right: The experimental imitation setup. A stereovision system tracks the two potential targets and the demonstrator's hand. The robot reach to the target to which the demonstrator is reaching.

the VITE models ($\mathbf{r_T}$ of equation 1). A picture of the experimental system is shown on Figure 6.

2.6 Application to imitation

Because the movement is fully specified by the target location and the current arm configuration and velocity, this model is easily applied for the imitation of reaching movements. Indeed, it has been showed that imitation is goal-directed [1]. Imitation can be obtained by deducing the target to which a demonstrator is reaching, and reach to this target as well. In order to have more reactive and natural interaction, the system can try to predict the target to which a human his reaching and start his movement before the end of he demontration. There are many ways to predict the target of the movement, the simplest and most robust being chosing, after the movement is well engaged, the target closest to the hand of the demonstrator. This has also been implemented on the robot, allowing reaching movement imitation games. Here again a stereovsion system tracks the hand of the demonstrator as well as the two potential targets. If the distance from the hdan to the closest target is below a given threshold, the robot reaches for this target. Figure 6, right shows a picture of the setup.

2.7 Discussion

The model described above allows a robust control of reaching movements, that can deal online with unexpected events such as hand or target displacement. In this model, two redundant controllers operate in parallel. This redundancy is exploited in order to achieve a better control. In that respect, this approach is similar to kernel methods [14], which perform a dimensionality augmentation in order to simplify a given problem.

Our model applies two basic principles suggested by the study of human movements. First it simultaneously involves information and computations in various modalities and frames of reference (vision and proprioception), and second it relies on a very robust dynamical system (the VITE model), which only considers goal-relevant variables and can thus handle all "perturbations" due to the competing modalities. Moreover, the principle of having the environment and self represented in the various modalities in a parallel way is consistent with recent experimental findings [8]. It is interesting to notice that in our model the redundancy of the 4-dofs arm is not a problem anymore, rather it is exploited to better satisfy the constraints within and across modalities.

Because the model is centered on the reaching target, it is very simple to use it in an imitation framework. The only necessary additional feature is to extract (or possibly predict) the goal from a demonstration. In a first step, this can be done very simply, but of course further developpements can be made in order to have a more intelligent, flexible and robust goal extraction.

3 University of Hertfordshire Contribution to task 5.2: Early Imitation Behaviours

During the first year of RobotCub University of Hertfordshire has started research into human-robot interaction experiments to contribute to task 5.2 “Early imitation behaviours” within WP5. Work in this area had only started in the second half of the first year and is thus summarized in this deliverable. The effort charged by University of Hertfordshire to the project during months 7-12 of the project is 2 PMs. Experiments are being designed with a child-sized robot called KASPAR. The robot has been developed as part of WP6 and is described in more detail in Deliverable 6.1. Human-robot interaction experiments with the robot will be performed during months 12-18 in order to contribute to task 5.2 as specified in the 18 months RobotCub implementation plan.
KASPAR is a 20 DOF child-sized humanoid suitable for research into low-level imitation mechanisms. At the date of submission of the deliverable only the head is operational, 2 arms are under development. We aim to approach imitation from a social and communicative and not a learning perspective as it is often taken in robotics research. The social perspective in robotics imitation research has been emphasized in [5]. The communicative perspective is in line with developmental psychology research on imitation [13] which is a primary source of inspiration for our work in RobotCub in developmental robotics. Interacting humans who are in agreement often unconsciously imitate each other, adopting the same pose or mirroring each other’s movements [12], and humans in any interaction tend to move their bodies synchronously with their, and with their partners, utterances [4], [11]. Imitation is most commonly perceived as a learning tool, but it is important to note that in this context the interaction partners are not using imitation to learn new skills but as a fundamental and non-verbal communicative device. We are interested in the relationship of imitation to synchronisation and kinesics between interaction partners and its place in propagating and regulating interaction dynamics.

3.1 HRI Research Platform KASPAR (cf. Deliverable 6.1)

KASPAR’s design rationale is to provide a research platform with the minimal degrees of freedom and realism required for rich interaction behaviour. Thus far an 8 degree-of-freedom head has been constructed and mounted on a child mannequin body. The head has 3 DOFs in the neck (rotate, pitch and tilt), 2 in the eyes (vertical and horizontal), 2 in the mouth (open and smile) and 1 in the eyelids (open and close). It has a humanoid appearance with a silicon rubber skin and minimal visible mechanical parts, but stops short of total realism. Two 4 DOF arms with 2 DOF hands are currently in development, and a PC/servo which will be used in developing a software control API.

3.2 Input Into RobotCub

It is anticipated that the algorithms arising from these studies will form part of the software control suite for the Cub, and provide basic communicative behaviours that will allow the scaffolding of more complex social interaction or imitative learning behaviour.

4 IST Contribution to task 5.2

The development of imitation capabilities requires an appropriate definition of the sequence of learning steps to reach that goal, as well as adequate performance evaluation methods to decide when to switch to higher developmental levels. In other words, it is important to define the overall hierarchy of developmental stages and the skills that must be acquired at each level. Table 1 shows the structure we adopt for the main developmental stages the robot (or a human infant, [16, 22]) will go through: (i) Learning about the self; (ii) Learning about objects and the world and (iii) Learning about others and imitation.
Each stage in the "developmental pathway" requires the acquisition of different sets of skills. The time line explains the restrictions governing the system. We do not distinguish between innate versus learned behavior in biological systems ("the nature versus nurture" question). Instead, we just request all the modules to be present before the system can develop to the next level.

Table 1: Developmental pathway for the Perceptual and Motor capabilities (in *italic* the modules that are learnt by the robot)

Time line	Perceptual/Motor Capabilities
↓ self-awareness	eye vergence random movements *Arm-head* coordination near-space mapping
↓ world-awareness	near-space mapping *visually initiated reaching* *visual control of grasp*
↓ imitation	detection of other's actions imitation of tasks

In the first developmental level, the robot acquires very simple and yet crucial capabilities: vergence control and object foveation/tracking. Then, by executing random arm movements, in a self exploratory mode, it begins to coordinate head and arm configurations, by creating a arm-head map. This map is accurate enough to allow for reaching and grasping objects in easy positions.
In the second developmental stage, the robot builds a map of the surrounding area (object positions and identification). Driven by attentional cues, the robot engages in more challenging grasping tasks, for which the previously learned arm-head map is not sufficiently accurate. For that reason we propose a novel method for visually controlled grasping, which improves over time and ensures the necessary robustness.
At the final developmental stage, the presence of a demonstrator will elicit a task imitation behavior, the actions are analyzed and replicated, according to a given metric. For this purpose, the system must be able to decompose the observed action into the relevant key elementary actions that must be executed.
The experiments described here were implemented with IST's humanoid robot, Baltazar, equipped with a $4\ dof$ binocular head, a $6\ dof$ arm and an $11\ dof$ (under-actuated by 4 motors) hand. The robot is shown in Figure 7 and described in detail in [21].

4.1 Self-Awareness

Understanding the structure of the near-space is very important, since it contains "reachable" objects and our own body. A method such as the one proposed in [17] can segment objects at different depths, by computing the disparity between images using different disparity channels.

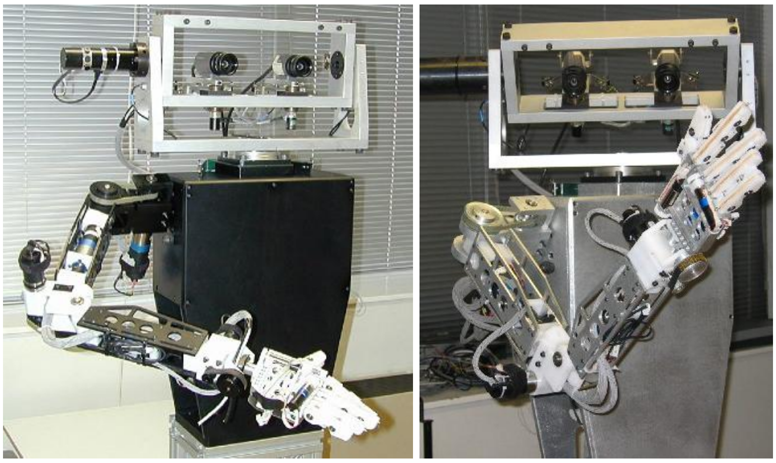

Figure 7: Left: Baltazar, a 14 degrees of freedom humanoid torso. Right: Head-hand coordination.

Many tasks need a very fine Arm-head coordination. Object manipulation is only possible with precise visual control of the hand. In order to coordinate Arm positions with Head position, we create an *Arm-Head Map*. This map is bidirectional. If the head position is fixed moving the arm to the mapped position puts the hand in the fovea of the two eyes. If the arm is fixed, we can visually locate it by moving the head to the mapped position.
The learning data set is gathered during self-observation. The arm is moved around in the space, while the hand is tracked and foveated. Figure 7 shows the hand being moved to the front of the eyes by using the *Head-Arm map*. The quality of this map is good enough to guarantee that the hand can be maintained inside image, but not necessarily in the fovea. In our experiments, the average error is about $5cm$, corresponding to 15% of the image.
This map allows the system to reach and, in special cases, grasp objects. This will be very motivating and in the next level object grasping will develop further.

4.2 World Awareness

As the robot gains control over its own perceptual and motor capabilities, it will get more and more interested in exploring its surrounding world. This exploratory motivation will call for the development of more advanced manipulative capabilities as opposed to the rudimentary skills available during phase one. The development path will require the following new skills: (i) detect object's positions in the nearby space and store this information in some sort of representation (near space map); (ii) learn how to reach objects in a controlled manner, using visual feedback, and grasp them.
There is neurological evidence of spatial aware neurons that are active when movement or objects are present near the skin [24]. It is also known in developmental psychology that infants became aware of the near and far space very early. It is very useful to know where an object is and whether or not it can be grasped. After all the time spent interacting with its own hand, the system can already distinguish objects at different depths (using vergence-based, depth segmentation) and search for the desired one.
Through exploration of the surrounding space, the robot creates a mental map of the existing objects, memorized in terms of head (proprioceptive) coordinates. In Figure 8 Baltazar is searching for "fruits" around him where different objects are assumed to have different colours.
At the first stage of development, the estimated *Arm-Head map* allows the system to (crudely) move the hand towards an object. The problem with this (open-loop) approach is the absence of a mechanism for error correction. This is the reason why babies in this phase restart the grasp quite often, instead of

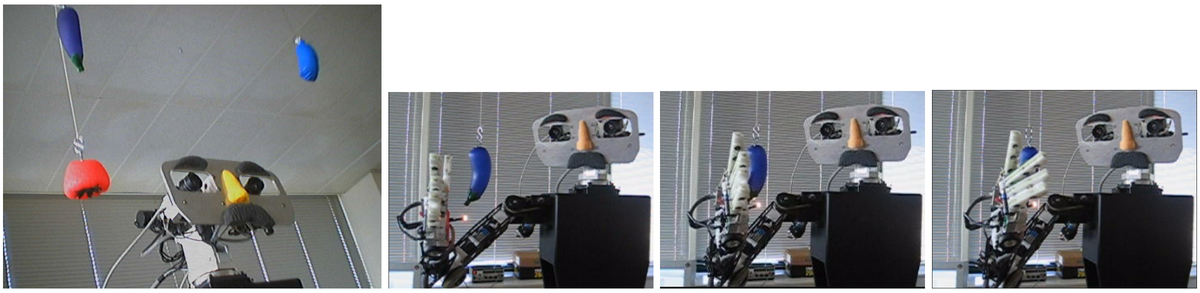

Figure 8: Left: mapping object positions in head coordinates. Right: several frames in the sequence from the initial position resulting from the *Head-Arm Map* followed by the visually guided part and object grasping.

correcting it [23].
The second stage of object reaching relies on visual feedback. The *Head-Arm map* is used to move the hand to the objects vicinity. Then, accurate positioning is achieved by visual guidance in closed loop. With this phase, it is possible to grasp objects in a reflex type manner, the hand closing after touch.
We adopted a visual servoing perspective, [19], with the system learning the image and robot Jacobians, [20]. The image *Jacobian* (J) relating image changes ($\Delta \mathbf{y}$) caused by motor movements ($\Delta\theta$), is iteratively estimated by:

$$\hat{J}(t+1) = \hat{J}(t) + \alpha \frac{\left(\Delta \mathbf{y} - \hat{J}(t)\Delta\theta\right)\Delta\theta^T}{\Delta\theta^T\Delta\theta}$$

where α denotes the Jacobian update rate. To move the system to the desired image position y^*, we apply the following control law:

$$\boldsymbol{\Delta}\theta = g\left(J^+\left(\mathbf{y}^* - \mathbf{y}\right)\right)$$

where J^+ represents the pseudo-inverse of J and the function $g(.)$ can be chosen to have a exponential, linear or any other type of convergence.
In order to deal with a larger workspace and to incorporate some open-loop movements, we improved the existing algorithm. Figure 8 shows the resulting behavior of the system while grasping objects. The hand is closed after sensing the contact with the object. Grasping fast moving objects will require learning some form of pre-shaping and predicting the time of contact with the object.

4.3 Imitation

Regarding imitation, our recent research addresses the problem of summarizing complex actions that the robot can learn how to perform afterwards. Figure 9 (left) shows an example of a task being executed. It consists of picking up some objects and moving them around. To imitate this task, the robot will first need to understand the spatial relations of objects around the demonstrator (far space).
Understanding the near space is necessary to establish correspondence between the demonstrator perspective its own (self) viewpoint (i.e. the blue object is on the left of the demonstrator, but it is in front of me). After the observation of the demonstration movements, the important task moments must be extracted and segmented. Finally the task is repeated by the robot, using the task description and all the modules previously learned.
The actions and movements of the demonstrator must be segmented and codified in a way useful for imitation. We developed a method consisting in a multiple object tracking and a “task point detector”. When doing manipulation our hand will very frequently occlude objects. Grasping and releasing can be very difficult to detect. Every object can have three movement ‘Â´states”: static, moving and being

moved. When an object is moving its velocity profile can be predicted with Newtonian dynamics, when being moved, it has the same velocity as the hand. The algorithm will mark every point in the trajectories of the objects that satisfy the following constraints: all object are static, the hand is not moving and the hand is not occluding any object.
The task is then codified by having objects with their physical properties (shape and color) and their spatial relations (A between B and C;A right of B or A left of B).

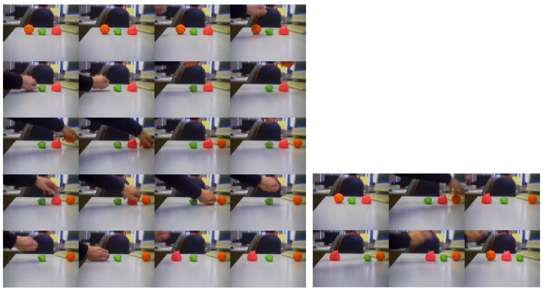

Figure 9: Left: Several frames of the task demonstration, involving a total of 234 frames. Right: Segmentation of a task into meaningful key images. Notice that from the third to the fourth image there is no difference in the ordering of the object, just their absolute distances. These relevant points where extract online from the original video sequence.

The complete sequence, shown in Figure 9, has 234 frames that were processed online for the automatic extraction of the task (key) points. We can see that the system succeeds in detecting which frames are important to describe the task.
As mentioned in [18], imitation goals are not always very clear. In our case the imitation task will proceed in order to have the same spatial relations. In case the demonstrator has made a movement and there is no difference in the ordering of objects (Figure 9), the robot will mimic the absolute spatial positions. We can see that all the modules developed until this point were essential to be able to replicate the task at hand.

4.4 Conclusions/Future Work

We have the current work at in the developmental route for a humanoid robot[1] to acquire increasingly more complex skills.
We described experiments and results in the different levels: self-awareness, world-awareness and social-awareness (imitation). The skill available to each level are built upon skills learned in previous developmental stages. Particular effort was devoted to the earlier aspects of visuomotor coordination and visual servoing for object grasping.
In the future, we will focus our efforts, together with other partners in RobotCub, on the aspects of learning the interaction between people and objects.

References

[1] H. Bekkering, A. Wohlschläger, and M. Gattis. Imitation of gestures in children is goal-directed. *The Quarterly Journal of Experimental Psychology*, 53A(1):153–164, 2000.

[2] C. von Hofsten, “Structuring of early reaching movements: A longitudinal study,” *Journal of Motor Behavior*, vol. 23, no. 4, pp. 280–292, 1991.

[1] see http://vislab.isr.ist.utl.pt/baltazar for videos showing the experiments in this work

[3] D. Bullock and S. Grossberg. Neural dynamics of planned arm movements: Emergent invariants and speed-accuracy properties during trajectory formation. *Psychological Review*, 95(1):49–90, 1988.

[4] W.S. Condon and W.D. Ogston. A segmentation of behavior. *Journal of Psychiatric Research*, 5:221–235, 1967.

[5] Kerstin Dautenhahn. Getting to know each other - artificial social intelligence for autonomous robots. *Robotics and Autonomous Systems*, 16:333–356, 1995.

[6] M. Desmurget, M. Jordan, C. Prablanc, and M. Jeannerod. Constrained and unconstrained movements involve different control strategies. *Journal of Neurophysiology*, 77:1644–1650, 1997.

[7] M. Desmurget, D. Pélisson, Y. Rosseti, and C. Prablanc. From eye to hand: Planning goal-directed movements. *Neuroscience and Biobehavioural Reviews*, 22(6), 1998.

[8] J.M. Hillis, M.O. Ernst, M.S. Banks, and M.L. Landy. Combining sensory information: Mandatory fusion within, but not between senses. *Science*, 298, 2002.

[9] N. Hogan. An organizing principle for a class of voluntary arm movements. *Journal of Neuroscience*, 4(11):2745–2754, 1984.

[10] J.A.S. Kelso. *Dynamic Patterns: The Self-Organization of Brain and Behaviour*. MIT Press, 1995.

[11] Adam Kendon. Movement coordination in social interaction: Some examples described. *Acta Psychologia*, 32:100–123, 1970.

[12] Marianne LaFrance. Posture mirroring and rapport. In Martha Davis, editor, *Interaction Rhythms: Periodicity in Communicative Behaviour*, chapter 13, pages 279–297. Human Sciences Press, Inc., New York, 1982.

[13] Jacqueline Nadel, Caroline Guerini, Ann Peze, and Christine Rivet. The evolving nature of imitation as a format for communication. In J. Nadel and G. Butterworth, editors, *Imitation in Infancy*, chapter 7. Cambridge University Press, 1999.

[14] B. Schölkopf and A. Smola. *Learning with Kernels*. The MIT Press, 2002.

[15] E. Todorov and M.I. Jordan. Optimal feedback control as a theory of motor coordination. *Nature Neuroscience*, 5(11):1226–1235, 2002.

[16] A. Arsénio. *Cognitive-Developmental Learning for a Humanoid Robot: A Caregiver's Gift*. PhD thesis, Massachusetts Institute of Technology, Boston, USA, Sept 2004.

[17] A. Bernardino and J. Santos-Victor. A binocular stereo algorithm for log-polar foveated systems. In *Biological Motivated Computer Vision*, Tuebingen, Germany, 2002.

[18] György Gergely, Harold Bekkering, and Ildikó Király. Rational imitation in preverbal infants. *Nature*, 415:755, Feb 2002.

[19] S. Hutchinson, G. Hager, and P. Corke. A tutorial on visual servo control. *IEEE Transactions on Robotics and Automation*, 12(5):651–670, October 1996.

[20] M. Jaegersand. Visual servoing using trust region methods and estimation of the full coupled visual-motor jacobian. In *IASTED Applications of Control and Robotics*, Orlando, EUA, 1996.

[21] M. Lopes, R. Beira, M. Praça, and J. Santos-Victor. An anthropomorphic robot torso for imitation: design and experiments. In *International Conference on Intelligent Robots and Systems*, Sendai, Japan, 2004.

[22] Lorenzo Natale. *Linking Action to Perception in a Humanoid robot: a Developmental Approach to Grasping*. PhD thesis, University of Genova, 2004.

[23] V. Gregory Payne and Larry D. Isaacs. *Human Motor Development: a Lifespan Approach*. Mayfield Publishing Company, California, USA, 4th edition, 1999.

[24] G. Rizzolatti, L. Fadiga, L. Fogassi, and V. Gallese. The space around us. *Science*, 277:190–191, 1997.